Available online at www.sciencedirect.com

ScienceDirect

Physics Procedia 66 (2015) 432 – 438

Physics Procedia

C 23rd Conference on Application of Accelerators in Research and Industry, CAARI 2014

Recent Fast Neutron Imaging Measurements with the Fieldable Nuclear Materials Identification System§

T. A. Wellington[a]*, B. A. Palles[a], J. A. Mullens[b], J. T. Mihalczo[b], D. E. Archer[b], T. Thompson[c], C. L. Britton[b], N. D. Bull Ezell[b], M. N. Ericson[b], E. Farquhar[b], R. Lind[b], J. Carter[a,b]

[a]*Bredesen Center for Interdisciplinary Research and Education, University of Tennessee, Knoxville TN 37996, USA*
[b]*Oak Ridge National Laboratory, Oak Ridge, Tennessee 37831, USA*
[c]*Cadre5, LLC, Knoxville, Tennessee 37932, USA*

Abstract

This paper describes recent fast-neutron imaging measurements of the fieldable nuclear materials identification system (FNMIS) under development by Oak Ridge National Laboratory with National Nuclear Security Administration (NNSA-NA-22) support for possible future use in arms control and nonproliferation applications. This paper presents initial imaging measurements performed at Oak Ridge National Laboratory with a Thermo Fisher API 120 DT generator and the fast-neutron imaging module of the FNMIS.

Selection and peer-review under responsibility of the Organizing Committee of CAARI 2014

Keywords: nonproliferation; arms control; DT neutron generators; fast neutron imaging; associated particle imaging

* Corresponding author. Tel.: +1-865-576-4720; fax: +1-865-576-8380.
E-mail address: twelling@vols.utk.edu

Selection and peer-review under responsibility of the Organizing Committee of CAARI 2014
doi:10.1016/j.phpro.2015.05.054

1. Introduction

Fast-neutron imaging with associated particle imaging DT generators was initiated at Oak Ridge National Laboratory (ORNL) in 2004 after feasibility calculations by James Mullens (Mullens, 2004). The evolution of the imaging systems since then is depicted in Fig. 1.

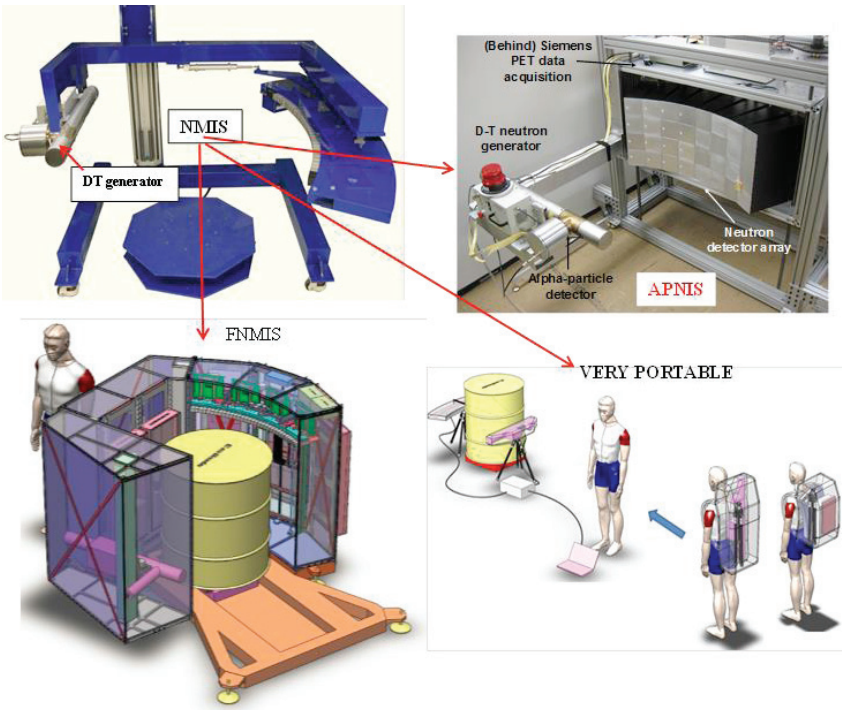

Fig. 1. Fast-neutron imaging systems at ORNL.

The initial imaging system, shown in the upper left of Fig. 1, added a tomographic imaging detector array to the Nuclear Materials Identification System (NMIS) that already employed fast-neutron coincidence measurements for active interrogation (Mullens, 2004). The array consisted of a single row of 32 2.5 cm × 2.5 cm imaging detectors that could be moved vertically with a DT generator that contained an embedded alpha detector. The pixelated alpha detector is used to determine the time and direction of those neutrons emitted towards the imaging detector array, due to the coincident emission of an alpha particle and neutron in essentially opposite directions via the DT reaction. Over the course of five years the system's imaging improved, as the detectors increased from 1 to 8 to 16 alpha detector pixels, while the imaging array grew from 8 to 32 detectors, and the imaging array was subsampled horizontally to boost the resolution from 32 to 128 effective detector positions. The Advanced Portable Neutron Imaging System (APNIS) (Blackston, 2009), shown in the upper right of Fig.1, evolved from NMIS and uses multiple rows of imaging detectors and alpha pixels. The system provides ~2.5 times better spatial resolution and has 3200 1 cm × 1 cm imaging detectors.

NMIS later evolved into a fieldable version shown in the lower left of Fig. 1 for the US Department of Energy (DOE) Office of Nuclear Verification (ONV-NA-243) and is designated as the Fieldable Nuclear Materials Identification System (FNMIS). System modifications include a lighter weight modular construction, lower power ASIC-based detector electronics, computer control of electronics settings to allow for both automation and streamlined user-operation A description of the ASIC electronics designed for FNMIS has been reported previously (Archer, 2010). Development work on this system started late in 2007 and is expected to be completed in 2015. FNMIS is currently managed by the DOE Office of Defense Nuclear Nonproliferation Research and Development

(NA-22). A concept for a more portable version for counter terrorism and other applications is depicted in the lower right of Fig. 1.

The NMIS, APNIS, and FNMIS systems are capable of transmission imaging (Mullens, 2004), induced fission imaging (Hausladen, 2010; Mullens, 2011), elastic scatter imaging (Grogan, 2012), and isotope identification with the addition of time-tagged gamma ray spectrometry (Archer, 2010).

This paper describes initial imaging measurements with the FNMIS using an Associated Particle Imaging (API) 120 DT neutron generator from Thermo Fisher.

2. Configuration of Materials

Measurements were performed on a spherical steel shell and on a cylindrically symmetric composite assembly composed of a polyethylene rod, a depleted uranium (DU) annular casting, iron pipes, and steel shot. Both objects are shown in Figure 2.

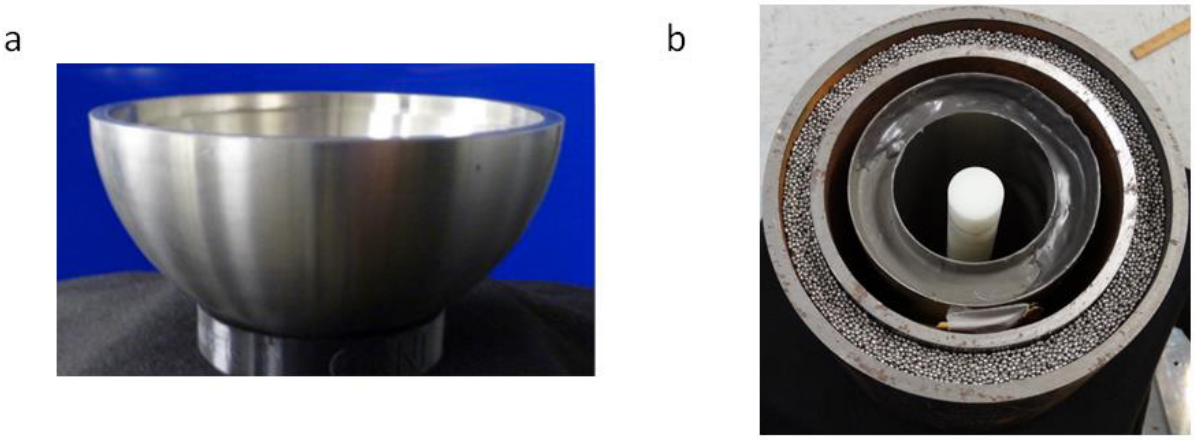

Fig. 2. (a) spherical steel shell; (b) composite assembly.

3. Measurements

Photographs of the hemispherical shell and the composite assembly in measurement position are shown in Fig. 3a and 3b. In both photographs the FNMIS imaging detector array is contained in the cabinet, opposite the neutron generator. The center of the shell is 23 cm from the DT generator neutron production spot, while the center of the composite assembly is located at 28 cm. The objects are placed closer to the generator to cast a larger neutron shadow on the imaging detectors, increasing their magnification in the final image to improve resolution.

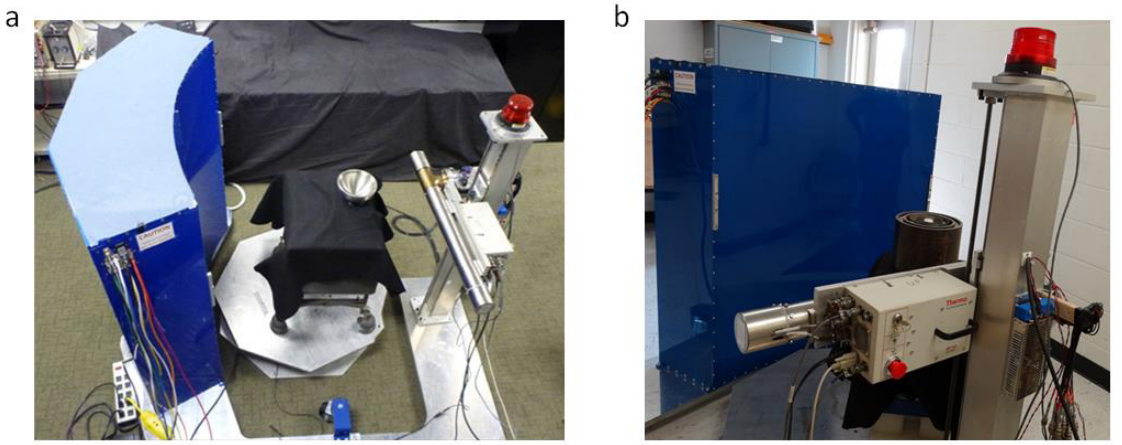

Fig. 3. FNMIS imaging measurement configuration with (a) spherical steel shell and (b) composite assembly.

3.1. Spherical Shell

The radiograph obtained by scanning the vertical imaging arm and imaging array vertically, from slightly below the steel shell to slightly above with the steel shell, is shown in Fig. 4a. Figure 4b shows tomographic images that show the horizontal slice through the shell at various heights. These images are reconstructed from the raw data using the industry-standard filtered back projection method. Since these images are derived from DT neutron transmission measurements, they are images of the 14.1 MeV neutron attenuation (interaction) cross sections of the materials present.

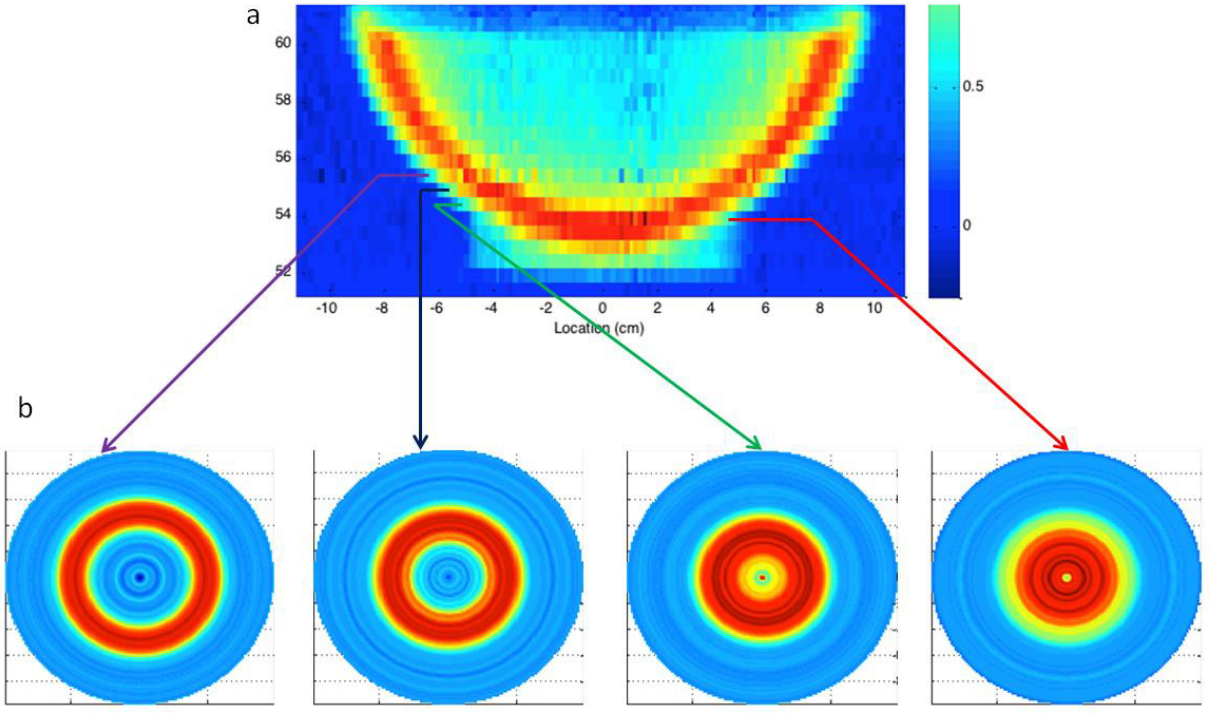

Fig. 4. (a) FNMIS radiograph of spherical steel shell; (b) cross-sectional filtered back projection image scans at different shell heights (specific location of scan noted by arrows).

These results were corrected for neutron scattering and used to estimate the dimensions and attenuation coefficients for the steel by fitting the measurement with a ray tracing algorithm. The object is modelled as a collection of shapes (e.g. hollow cylinders). The dimensions of these shapes (e.g. diameters) and the neutron attenuation (total cross section) of each shape is a variable to be determined by an optimal fit of the model to the object measurement. The ray tracing algorithm simply integrates the object's attenuation of the neutrons passing through it. A nonlinear fitting algorithm in the Matlab software drives the iterative solution which finds the values of dimensions and attenuations that give the optimal fit of the ray trace model to the measurement. The fitted results and the actual dimensions are given in Table 1. The results show a good match between the fitted and the measured data.

Table 1. Comparison of the measured results with the actual dimension and attenuation coefficient for the steel shell.

	Fitted	Actual
Inner diameter (cm)	15.0	15.0
Outer diameter (cm)	17.8	17.6
Thickness (cm)	1.40	1.33
Attenuation coefficient (cm^{-1})	0.210	0.220

3.2. Composite Assembly

The filtered back projection image for the composite assembly was obtained by positioning the vertical imaging arm 88.5 cm above the ground and 28 cm from the neutron production spot location. The filtered back projection image is compared to the photograph in Fig. 5.

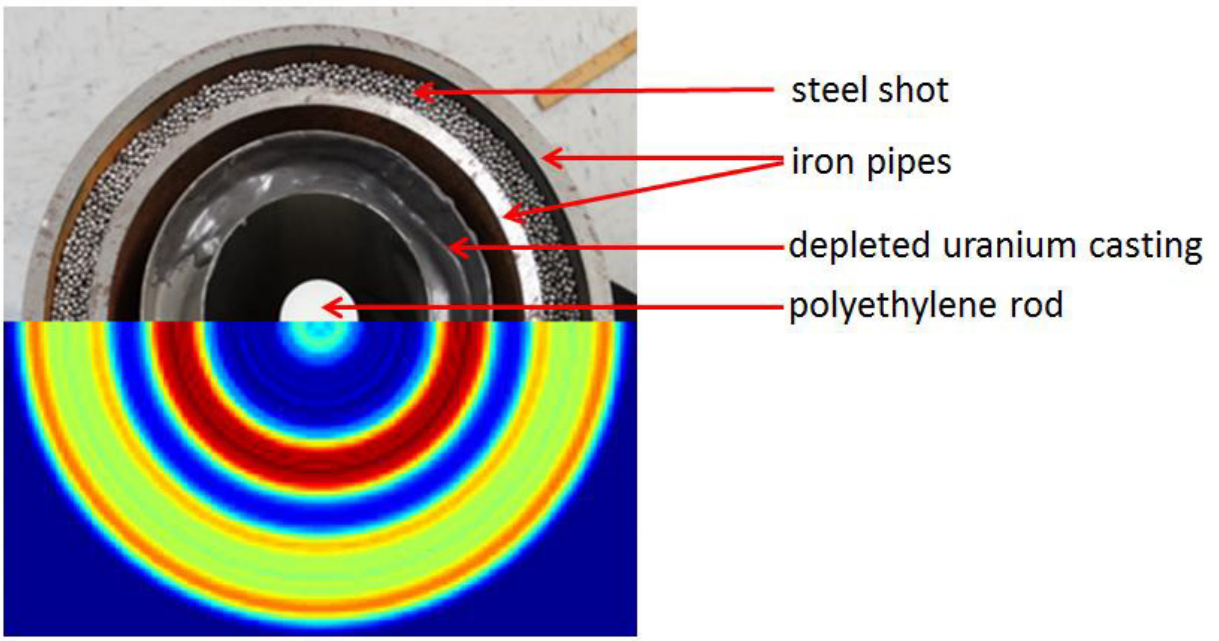

Fig. 5. Comparison of filtered back projection image with photograph of configuration.

These results were also corrected for neutron scattering, and the dimensions and attenuation coefficients for each object in the assembly were obtained from a ray tracing model fit to the measurement as it was done for the

spherical shell. The measurement datum used is the attenuation projection, that is, the total attenuation along each path between the DT neutron source and an imaging detector ("detector slot"), which correlates to the lateral position within the object. Figure 6 shows a graphical comparison of the measured data and the ray tracing algorithm fit to that data. The fitting results and the actual dimensions for each object are given in Tables 2–6. The results show that the fitting was successful for each component of the assembly.

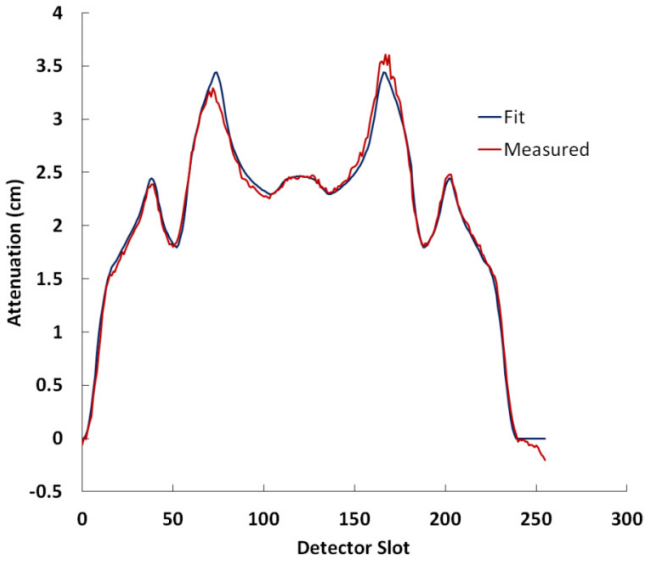

Fig. 6. Comparison of fitted and measured data.

Table 2. Comparison of the measured results with the actual dimension and attenuation coefficient for polyethylene rod.

	Fitted	Actual
Diameter (cm)	2.58	2.54
Attenuation coefficient (cm^{-1})	0.100	0.110

Table 3. Comparison of the measured results with the actual dimension and attenuation coefficient for the depleted uranium casting.

	Fitted	Actual
Inner diameter (cm)	8.52	8.89
Outer diameter (cm)	12.6	12.7
Attenuation coefficient (cm^{-1})	0.250	0.280

Table 4. Comparison of the measured results with the actual dimension and attenuation coefficient for the steel shot.

	Fitted	Actual
Inner diameter (cm)	16.9	16.8
Outer diameter (cm)	20.4	20.3
Attenuation coefficient (cm^{-1})	0.140	0.130

Table 5. Comparison of the measured results with the actual dimension and attenuation coefficient for the small iron pipe.

	Fitted	Actual
Inner diameter (cm)	15.4	15.2
Outer diameter (cm)	16.9	16.8
Attenuation coefficient (cm^{-1})	0.180	0.220

Table 6. Comparison of the measured results with the actual dimension and attenuation coefficient for the large iron pipe.

	Fitted	Actual
Inner diameter (cm)	20.4	20.3
Outer diameter (cm)	22.0	21.9
Attenuation coefficient (cm^{-1})	0.170	0.220

4. Conclusion

The initial measurements have demonstrated satisfactory imaging performance of the new FNMIS imaging detector module. The inadequacies in the fits are attributed to the imperfect scattering correction that has been previously reported (Grogan, 2010). Neutron scatter, especially small-angle neutron scatter, effectively blurs the measured image. The ray tracing algorithm does not model neutron scatter so the model fit tries to compensate by varying the shape dimensions and attenuation, leading to some distortions of the image. The overall attenuation profile of the collection of objects is fitted well by the model (~5% error). The fit for the individual objects show more variation since the fit method can trade off dimension and attenuation errors in multiple objects to achieve a better fit to the measurement of the composite object.

Acknowledgements

This research is supported by the National Nuclear Security Administration, Defense Nuclear Nonproliferation, Office of Nonproliferation and Verification Research and Development under contract with UT-Battelle, LLC.

References

Archer, Daniel E., Britton Jr., Charles L., Carter, Robert J., Lind, Randal F., Mihalczo, John T., Mullens, James A., Radle, James E., Wright, Michael C., 2010. Fieldable Nuclear Material Identification System, Proceedings of the Institute of Nuclear Materials Management (INMM) Annual Meeting, Baltimore, MD, USA.

Blackston, M. A., Hausladen, P., Bingham, P. R., Erickson, M. N., Fabris, L., McConchie, S., Mihalczo, J. T., and Mullens, J. A., 2009. Using Fast Neutrons to Image Induced Fissions, IEEE Nuclear Science Symposium, Orlando FL.

Hausladen, P., Blackston, M., Mullens, J. A., McConchie, S., Mihalczo, J., Bingham, P., Ericson, N., and Fabris, L., 2010. Induced-Fission Imaging of Nuclear Material, Proceedings of the Institute of Nuclear Materials Management (INMM) Annual Meeting, Baltimore, MD.

Grogan, Brandon. "The Development of a Parameterized Scatter Removal Algorithm for Nuclear Materials Identification System Imaging," Diss. U of Tennessee, Knoxville, 2010. Web. 17 Dec. 2014.

Grogan, B., and Mihalczo, J. T., 2012. Identification of Lithium Isotopes using time tagged neutron scattering,Proceedings of the Institute of Nuclear Materials Management (INMM) Annual Meeting, Orlando, FL.

Mihalczo, John T., Mullens, James A., Mattingly, J. K., Valentine, T. E., 2000. Physical description of nuclear materials identification system (NMIS) signatures. Nucl. Inst. & Meth. In Phs. Res. A 450, 531–555.

Mullens, James A., Mihalczo, John, Bingham, Philip, 2004. Neutron and Gamma Ray Imaging for Nuclear Materials Identification, Proceedings of the Institute of Nuclear Materials Management (INMM) Annual Meeting, Orlando, FL.

Mullens, J. A., McConchie, S., Hausladen, P., Mihalczo, J., Grogan, B., and Sword, E., 2011. Neutron Radiography and Fission Mapping Measurements of Nuclear Materials with Varying Composition and Shielding, Proceedings of the Institute of Nuclear Materials Management (INMM) Annual Meeting, Palm Desert, CA.